Sieverts Law Empirical Exponent for Pd-Based Membranes: Critical Analysis in Pure H_2 Permeation

Alessio Caravella,[†] Francesco Scura,[†] Giuseppe Barbieri,*[,†] and Enrico Drioli[†,‡]

Institute on Membrane Technology (ITM-CNR), National Research Council, c/o The University of Calabria, Cubo 17C, Via Pietro Bucci, 87036 Rende CS, Italy, and Department of Chemical and Materials Engineering, The University of Calabria, Cubo 44A, Via Pietro Bucci, 87036 Rende CS, Italy

Received: January 23, 2010; Revised Manuscript Received: March 28, 2010

In this paper, the physical meaning of the Sieverts-type driving force exponent n is analyzed for hydrogen permeation through Pd-based membranes by considering a complex model involving several elementary permeation steps (adsorption on the membrane surface on the feed side, desorption from the surface on the permeate side, diffusion through the metal lattice, and the two transition phenomena surface-to-bulk and bulk-to-surface). First, the characteristic driving force of each step is evaluated, showing that adsorption and desorption singularly considered and the adsorption and desorption considered at the same time are characterized by driving forces depending on the ratio of feed and permeate hydrogen pressure. On the contrary, the diffusion step is found to present a driving force that is composed of two terms, one which corresponds to the original Sieverts law (with an exponent of 0.5) and the other which is the product of the pressure difference and a temperature-dependent factor. Then, the characteristic n is evaluated by applying the multistep model to two different membranes from the literature in several cases, (a) considering each permeation step as the only limiting one and (b) considering the overall effect of all steps. The results of the analysis show that for a low temperature and thin membrane thickness, the effect of the surface phenomena is, in general, a decrease of the overall exponent n toward values lower than 0.5, even though, under particular operating conditions, the n theoretical value of the surface phenomena is equal to unity. At a higher temperature and thickness (diffusion-controlled permeation), n tends to 0.5, even though the rapidity of this tendency depends strictly on the membrane diffusional parameters. In this frame, the expression developed for the diffusion step provides a theoretical reason why n values higher than 0.5 are found even for thick membranes and high temperature, where diffusion is the only rate-determining step.

1. Introduction

The interest toward the Pd membranes and its alloys has been increasing in the last two decades because it is known that this type of membrane is permeable to only hydrogen. This allows their use in those reactive processes that are favored by selective hydrogen removal, that is, steam re-forming of hydrocarbons, water−gas shift, dehydrogenation reactions, and others.[1] The particular properties of the Pd-based layer are due to the hydrogen permeation mechanism of solution-diffusion-type, which involves several steps. When the diffusion of the atomic hydrogen through the metal bulk of the membrane is the rate-determining step and the hydrogen concentration in the Pd-based lattice is lower enough than 1, the Sieverts law should be valid,[2,3] which identifies the difference of the hydrogen partial pressure square roots as the permeation driving force (eq 1).

$$J_{H_2} = \pi_{H_2}[\sqrt{P_{H_2}^{Feed}} - \sqrt{P_{H_2}^{Permeate}}] \quad (1)$$

This equation is very useful thanks to its simplicity, and for this reason, in the literature, its modified version (the Sieverts-type expression, represented by eq 2) is very often utilized to evaluate the hydrogen flux even when the diffusion is not the only rate-determining step.

$$J_{H_2} = \pi_{H_2}^{(n)}[(P_{H_2}^{Feed})^n - (P_{H_2}^{Permeate})^n] \quad (2)$$

The empirical exponent n in eq 2 is usually evaluated by means of a nonlinear regression. There are many papers in the literature where this exponent has been considered to establish which steps control the overall permeation process. In doing that, two problems should be faced. First, the permeation test should be sufficiently accurate to be sure that an eventual deviation from the Sieverts law is not caused by the inevitable experimental errors. Second, the crucial question arises whether a unique value of the n exponent could provide an unequivocal response concerning the membrane behavior.

The first question is only addressed to the capability of the experimentalist, who should avoid tests involving a hydrogen mixture since the external mass transfer under certain conditions (concentration polarization) could be relevant[4] and hide some important aspects. In this field, the role of the experimental errors during the permeation test can be relevant and even crucial. Regarding the second question, it must be emphasized that values of the n exponent higher than 0.5 (commonly ranging between 0.5 and 1) are usually explained by the effect of surface phenomena that influence the permeation. However, in some cases, the deviation is observed also for quite thick membranes

* To whom correspondence should be addressed. E-mail: g.barbieri@itm.cnr.it or giuseppe.barbieri@cnr.it. Fax: +39 0984 402103.
[†] National Research Council.
[‡] Department of Chemical and Materials Engineering, The University of Calabria.

10.1021/jp1006582
Published on Web 04/19/2010

(>50 μm),[5] for which there is no doubt that the diffusion through the Pd-based bulk controls almost completely the permeation process. A possible explanation for this deviation can be found in the different thermomechanical history of the membrane. That is why two membranes with the same thickness, alloy composition, and subject to the same operating temperature can exhibit very different permeance values. In evaluating the exponent n, its meaning has to be investigated in relation to the membrane properties. For example, if the membrane selectivity is not infinite (see, for instance, the papers of Hu et al.,[6] Guazzone et al.,[7] and Gielens et al.[8]), the effect of other diffusional mechanisms (like the Knudsen-type one) could be relevant. Therefore, in this case, the exponent value cannot be used to analyze the intrinsic membrane behavior. In other works, when infinitely selective membrane are considered,[9–12] some considerations about the rate-determining step can be drawn from the exponent, but this information should be coupled and analyzed together with the overall activation energy of the permeance. A low value of the activation energy (<∼30 kJ mol_H^{-1}) indicates that the surface phenomena of dissociative adsorption and recombinative desorption do not provide significant influence on the permeation process since they are characterized by a quite higher activation energy (∼54−146 kJ mol_H^{-1}).[13] In this direction, the aim of this paper is to investigate the intrinsic meaning (if any) of the n exponent of the Sieverts-type flux relation for infinitely selective Pd-based membranes. To do that, the hydrogen permeating flux will be evaluated by means of the elementary step model already described in refs 2 and 3 (and here recalled in the Appendix A). The so-obtained flux values (left-hand side of eq 3) will be equated to a phenomenological Sieverts-type expression (right-hand side of eq 3) involving the n exponent and corresponding permeance.

$$J_{H_2}\left(\begin{array}{c}\text{Solution of model}\\ \text{with elementary steps}\end{array}\right) = \pi_{H_2}^{(n)}[(P_{H_2}^{Feed})^n - (P_{H_2}^{Permeate})^n] \quad (3)$$

The present analysis will be applied to two membranes from the literature,[10,16] for which the model will be numerically solved by evaluating the corresponding diffusional parameters. In particular, the n values will be related to the several permeation steps considered, adsorption, desorption, diffusion in the Pd-based layer, and the two transitions named surface-to-bulk and bulk-to-surface, for each of which a driving force will be achieved, even considering the surface phenomena that limit the permeation at the same time (eqs 4−9). The form of these driving forces will allow one to establish whether the n exponent has a physical meaning in the operating conditions considered. Moreover, only hydrogen will be considered in this paper as the presence of external phenomena (polarization and inhibition) could hide the true intrinsic membrane behavior.

2. Description of the System

The system studied in this paper is represented in Figure 1, where three zones can be distinguished, the feed side, the membrane, and the permeate side. In the first and last zones, pure hydrogen is considered (no external mass transfer). On the contrary, some hydrogen profiles are established through the membrane because of the resistances to the flux due to the different steps composing the overall permeation process. These steps, reported in Figure 1, have been already considered in the paper of Ward and Dao[2] and in the ones of Caravella et al.,[3,4] who additionally studied the influence of a multilayered porous support[3] and the effects of the concentration polarization.[4] However, as said before, any effect of external resistance is here excluded. In addition to the permeation steps, in Figure 1, the corresponding variables characterizing the driving force of each step are indicated; on each side of the membrane, there are the hydrogen pressure P, the surface coverage θ, and the atomic hydrogen concentration in the lattice ξ, which are distinguished by subscripts indicating the feed (F) or permeate side (P).

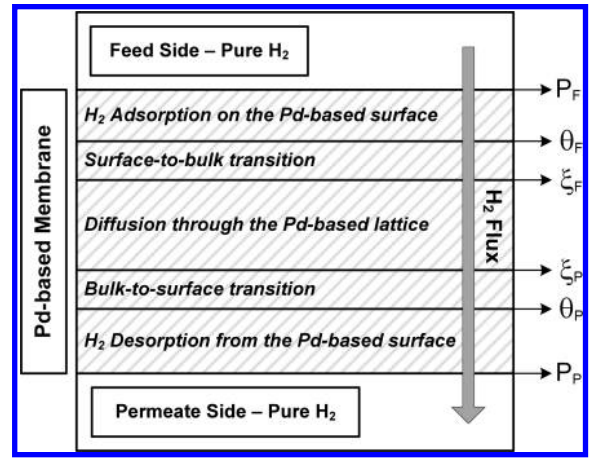

Figure 1. Sketch of the permeation steps considered in this paper.

TABLE 1: Functionality of the Hydrogen Flux with the System Variables in Each Permeation Step (see Appendix A)

steps	expression of the permeating flux
adsorption	$J_{H_2} = f_1(P_F,\theta_F)$ (see eq 16)
surface-to-bulk	$J_{H_2} = f_2(\theta_F,\xi_F)$ (see eq 20)
diffusion	$J_{H_2} = f_3(\xi_F,\xi_P)$ (see eq 25)
bulk-to-surface	$J_{H_2} = f_4(\xi_P,\theta_P)$ (see eq 21)
desorption	$J_{H_2} = f_5(\theta_P,P_P)$ (see eq 17)

According to this notation, the flux in the adsorption step is a function of P_F and θ_F, the one in the surface-to-bulk transition is a function of θ_F and ξ_F, and so on (Table 1). In the next section, the driving force characterizing each permeation step will be evaluated by expressing the nondirectly measurable variables (θ and ξ) as functions of the hydrogen pressure of the feed and permeate side.

3. Theoretical Driving Force of Each Single Permeation Step

As mentioned in the Introduction, in order to be able to characterize the membrane behavior in permeation tests, it is necessary to discover the driving force characterizing the process in such a way for the permeance to be representative of what occurs inside of the membrane subject to permeation. To do that, all of the equations considered in the here-used complex model will be rewritten by adopting certain simplifying but reasonable hypotheses that allow the permeation laws of each step to be expressed in terms of hydrogen pressure on the feed and permeate sides. In the next subsections, these permeation laws and their implications will be deeply discussed, reporting in the Appendix A the details of the way in which the various expressions were obtained.

3.1. Adsorption-Limited Permeation Law. The first step investigated is the dissociative adsorption on the membrane surface. In this case, the variables of interest are the pressure on the feed side and the surface coverage of the dissociated hydrogen θ. The only hypothesis in the achievement of this permeation law is that θ is very close to 1. Actually, the numerical simulation always provides values of θ higher than 0.99 under the operating conditions considered; hence, this

hypothesis can be done without obtaining large errors. Using this consideration in the equation that expresses the adsorption-limited flux and considering the other permeation steps at the equilibrium, eq 4 is obtained (see eq 30 in Appendix A).

$$J_{H_2}^{Ads} = \pi_{H_2}^{Ads}(T)(\phi - 1) \tag{4}$$

$$\phi \equiv \frac{P_F}{P_P} \tag{5}$$

This equation is characterized by two terms, a permeance $\pi_{H_2}^{Ads}$, which is only a function of temperature, and a second term $(\phi - 1)$, the driving force, which is only a function of the hydrogen pressures. Here, two aspects are to be emphasized. First, the permeance is actually the kinetic constant of the reassociative desorption rate, which is described by an Arrhenius-type expression. Second, the characteristic driving force is not the simple difference of pressures but a little bit more complex expression depending on the pressure ratio. This result is very important since, to the authors' knowledge, this is the first time that this kind of driving force is identified for the adsorption-limited permeation. Actually, as said before, the flux expressions recalled in Table 1 are the same as the ones used by Ward and Dao in their model,[2] except for the flux of the hydrogen diffusion through the Pd-based bulk. However, in that work, the authors did not investigate the aspects related to the overall driving forces corresponding to each permeation step. Anyway, the particular form of this driving force, which is very different from a Sieverts-type expression, raises a question concerning the effective significance of the exponent n since it is not possible to know a priori if this driving force can be approximated under certain hypotheses by an empirical Sieverts law. An answer to this question will be found from a numerical point of view in the Result and Discussion section.

3.2. Surface-To-Bulk- and Bulk-to-Surface-Limited Permeation Law. Analogous to what was done for the adsorption, in this section, the permeation laws obtained for the two transitions surface-to-bulk and bulk-to-surface are shown. With respect to the previous case, in addition to the hypothesis of surface coverage very close to 1, another one was used, that is, that the atomic hydrogen concentration ξ in the Pd-based bulk is much less than 1. This one is a good approximation, too, since the maximum value obtained from the calculation for ξ is about 0.04, which surely fulfills the hypothesis requirement. Following an evaluation procedure analogous to the adsorption case, two identical expressions are obtained for both of the fluxes (see eq 33 in Appendix A)

$$J_{H_2}^{SB} = J_{H_2}^{BS} = \pi_{H_2}^{SB}(T)[P_F^{0.5} - P_P^{0.5}] \tag{6}$$

Therefore, for this permeation step, the model foresees the original Sieverts-type behavior. This fact will be confirmed later in the paper, when the driving force will be determined by means of a regression analysis of the data coming from the exact solution of the model equations.

3.3. Diffusion-Limited Permeation Law. The most important permeation step to be investigated is surely the diffusion through the Pd-based bulk. In fact, under the usual operating conditions, in which this type of membrane is used, the diffusion step is responsible of the majority of the pressure loss. That is why in many experimental works of the literature empirical driving force exponents not so far from 0.5 are found. As reported in Table 1, the variables playing a role in the diffusion-limited flux are the atomic hydrogen concentrations at the feed and permeate sides of the metal lattice, that is, ξ_F and ξ_P, respectively. Expressing these two variables in terms of the feed and permeate pressures analogously to what was done for the other steps, eq 7 is obtained (see eq 37 in Appendix A).

$$J_{H_2,lim}^{Diff} = \pi_{H_2}^{Diff}(T, \delta^{Mem})\left[(P_F^{0.5} - P_P^{0.5}) + a(T)\left(\frac{1}{2} + \frac{b}{T}\right)(P_F - P_P)\right] \tag{7}$$

As in the case of the surface-to-bulk and bulk-to-surface steps, also here, the hypothesis of $\xi \ll 1$ was used. This hypothesis, acceptable for the same reasons as the ones discussed in the previous subsection, allows the diffusion-limited characteristic driving force to be recognized. In this expression, it is possible to distinguish two contributions, the first one, which is characterized by the usual Sieverts driving force, and the second one, which depends on the simple difference of pressures premultiplied by two temperature-dependent terms taking into account the nonideal behavior of the metal lattice during the hydrogen permeation. These two contributions allow one to clearly show the theoretical reason why for some membranes, a driving force exponent a higher than 0.5 is found (see, for example, Peters et al.[10]). In fact, qualitatively speaking, this type of driving force provides, in general, an overall exponent between 0.5 and 1, even if it is not possible to express analytically this overall exponent as a function of the other two due to their intrinsic nonlinearity.

In the literature, the discrepancy from the original Sieverts exponent in pure hydrogen tests is sometimes explained by hypothesizing the presence of a certain influence of the surface phenomena, even at high temperatures (>∼400 °C) and thicknesses. However, the gap is found also for very thick membranes (>50 μm),[14] for which it is sure that the only contribution to the permeation is the one of the diffusion in the lattice. Therefore, the usefulness of eq 7 consists of providing a direct physical meaning to the discrepancy from the exponent of 0.5.

3.4. Desorption-Limited Permeation Law. Applying the same procedure as the one adopted for the adsorption step, an analogous result is found for the desorption step (eq 8), which provides a permeance identical to the adsorption one. However, in this case, the permeation driving force is different, it being dependent on the ratio between the permeate and feed pressure rather than on its inverse (see eq 40 in Appendix A).

$$J_{H_2}^{Des} = \pi^{Des}(T)\left(1 - \frac{P_P}{P_F}\right) = \pi^{Des}(T)\frac{1}{\phi}(\phi - 1) \tag{8}$$

This expression indicates a quite important aspect: if the permeate stream is kept in vacuum at very low pressure with respect to the feed side, the flux is not dependent on the driving force. In other words, this represents the definition of a simple method to check if the membrane is desorption-controlled under the operating conditions considered. Incidentally, also here, the representation of the desorption-limited permeation law by a Sieverts-type expression is questionable.

3.5. Adsorption−Desorption-Limited Permeation Law. The last case analyzed considers a situation in which both the surface phenomena of adsorption and desorption control at the same time the permeation process while all of the other steps

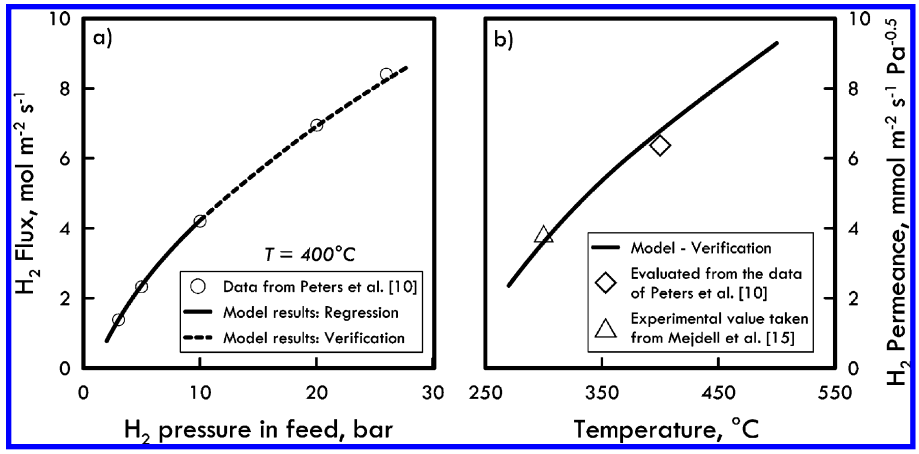

Figure 2. Comparison between the present model and some experimental data (a) in terms of H_2 flux as a function of H_2 pressure in feed at 400 °C (from Peters et al.[10]) and (b) in terms of H_2 permeance as a function of temperature (Peters et al.[10] and Mejdell et al.[15]). $P^{Perm} = 101.3$ kPa. $\delta^{Mem} = 2$ μm.

TABLE 2: Diffusional Parameters Used in the Simulation, Some of Which Were Obtained by a Nonlinear Regression of the Experimental Data Taken from the Experimental Work of Peters et al.,[10] Mejdell et al.,[15] and Barbieri et al.[16] [a]

diffusional parameters	membrane of Peters et al.[10]	membrane of Barbieri et al.[16]
D_H^0, m^2 s^{-1}	290×10^{-9}	94.5×10^{-9}
	taken from Holleck[17] and verified by data from Mejdell et al.[15]	calculated from the data of Barbieri et al.[16]
E_{Diff}, J mol^{-1}	22 175	14 175
	taken from Holleck[17] and verified by data from Mejdell et al.[15]	calculated from the data of Barbieri et al.[16]
b, K	1140	214
	calculated from the data of Peters et al.[10]	calculated from the data of Barbieri et al.[16]

[a] The parameters of Holleck were set to be constant in the simulation of the membrane of Peters et al.

are at the equilibrium. The two fluxes of adsorption and desorption must be equal for the condition of steady state; hence, only one expression has to be achieved.

Under the usual hypothesis of θ very close to 1, the expression represented in eq 9 is obtained, where the permeance is the same as the one evaluated when the two steps were individually considered (see eq 46 in Appendix A).

$$J_{H_2}^{AdsDes} = \pi^{AdsDes}(T)\left(\frac{P_F - P_P}{P_F + P_P}\right) = \pi^{AdsDes}(T)\frac{1}{\phi + 1}(\phi - 1) \quad (9)$$

Looking at the form for the particular driving force, it is possible to express it in a Sieverts-type law only in one case, that is, when particular operating conditions are chosen in such a way that the sum of the pressures of the feed and permeate sides is kept constant. In this case, the n value is evidently 1 and, analogously to the previous steps, this fact can help the user to understand if the membrane behavior is limited by the surface phenomena. In the next section, all of the theoretical equations obtained for each step-limited permeation will be verified and analyzed by solving them numerically in order to confirm the hypotheses according to which these equations were achieved.

4. Results and Discussion

4.1. Evaluation of the Diffusional Parameters. Once the characteristic permeation laws of the different steps considered were found, they were applied in the study of three real systems. In particular, three membranes from the literature were selected and used to evaluate the kinetic parameters necessary in the simulation, the experimental works of Peters et al.,[10] Mejdell et al.,[15] and Barbieri et al.[16] Concerning the work of Peters et al.,[10] the authors mainly investigated the behavior of a Pd−Ag membrane in a mixture in order to study the influence of the concentration polarization and CO inhibition. However, in the frame of this paper, the analysis is issued to the pure hydrogen test performed in their work, whose experimental values, together with the model curve, are reported in Figure 2a as functions of the feed pressure. In this analysis, the first three points were used to calculate the parameter b in eq 7, which takes into account the nonideal thermodynamic behavior of the system, whereas the last two points (the ones at high pressures) were used to confirm the model behavior.

The value of this parameter (see Table 2) was obtained by using a nonlinear regression, whose correlation coefficient R^2 exceeds the value of 0.99. The very good accordance between experiments and the model even at high pressure provides a certain indication of the goodness of the model. Regarding the parameters related to the diffusion coefficient, that is, the pre-exponential factor D_H^0 and the activation energy of the diffusion coefficient through the metal lattice E_{Diff} (eq 7), they were taken from the literature (from Holleck[17]) and set as constants in the simulation. The reason for this is that, in their paper, Peters et al.[10] investigated the hydrogen permeation at only one temperature (400 °C), whereas at least two temperatures are necessary to evaluate the parameters of an Arrhenius-type expression. Therefore, the only parameter that was possible to evaluate is the coefficient b. However, the goodness of this choice was verified by comparing the results calculated by simulation at 300 °C to the ones taken from the experimental work of Mejdell et al.,[15] where the authors considered almost the same type of membrane at 300 °C (Mejdell et al.[15] Table 3, sample 1C). In that work, a membrane permeability of 7.7 nmol m^{-1} s^{-1} Pa$^{-0.5}$ was found, which corresponds to a permeance of about 3.85 mmol m^{-2} s^{-1} Pa$^{-0.5}$ for a thickness of 2 μm. The quality of the overall accordance between the experimental data considered and the model results is shown in Figure 2b.

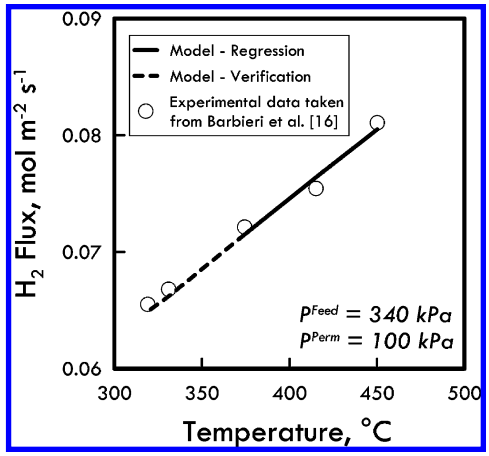

Figure 3. Comparison between the present model and some experimental data taken from Barbieri et al.[16] in terms of H_2 flux as a function of temperature; $P_F = 340$ kPa, $P_P = 100$ kPa. $\delta^{Mem} = 60$ μm.

The other experimental work considered in the model validation is the paper of Barbieri et al.,[16] from which the data of flux as a function of temperature were opportunely selected and reported here in Figure 3 together with the model curve. Analogously to what was done before, some points (the last three) were used for the calculation of the parameters, and other ones (the first two) were used for verification. Also in this case, the accordance with the experimental data is good, and furthermore, it was possible to evaluate all three diffusional parameters involved in eq 7. The overall results of the validation are reported in Table 2 in terms of used and calculated parameters. Throughout this paper, both of the membranes (Peters and Barbieri) will be considered in order to emphasize the differences and the analogies due to the different values of the diffusional parameters.

4.2. Simulation Results. In the present analysis, the role of each permeation step is individually investigated in order to identify its characteristics in terms of the permeation driving force exponent. Once the peculiarities of the single permeation steps show up, their influence on the membrane behavior will be analyzed by relating the single effects on the overall permeation rate.

The first step investigated is the diffusion of the atomic hydrogen through the Pd-based layer. From this point on, this step will be referred to as only "diffusion", without specifying anymore that it occurs in the selective layer. In Figure 4, the R^2 regression coefficient is reported for this step as a function of the driving force exponent for different temperatures and diffusional parameters, these last ones taken from the data of the experimental works of Peters et al.[10] (Figure 4a) and Barbieri et al.[16] (Figure 4b), respectively. The role of these parameters, (i.e., the pre-exponential factor D_H^0 and the activation energy E_{Diff} of the diffusion coefficient and the parameter b) was already described qualitatively in the previous section concerning the expressions of the limiting fluxes. However, a quantitative analysis is necessary to show the distance (if any) from the original Sieverts law in the two cases considered. Taking into consideration the first case (Figure 4a), it is possible to notice that each curve presents a maximum point, from which the optimal value of the exponent n is found. From these plots, it is shown that the R^2 values have a quite low sensitivity toward the n values. In fact, a variation of n of 0.1 (from ~0.45 to 0.55) is contained within an R^2 variation of only 5×10^{-4}, which would make one suppose that all of these values of n are actually equivalent to each other.

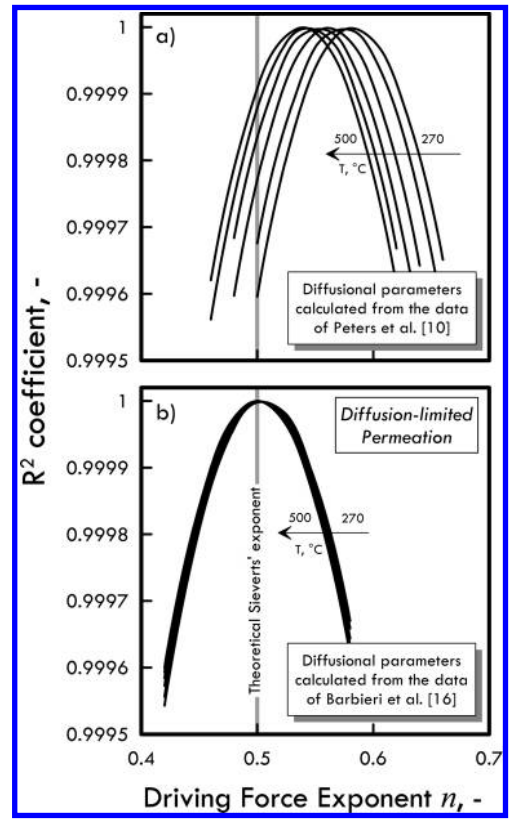

Figure 4. R^2 regression coefficient as a function of the driving force exponent in the case of diffusion-limited permeation for different temperatures. Diffusional parameters evaluated from the data of (a) Peters et al.[10] and (b) Barbieri et al.[16]

However, these data are obtained from simulation and, hence, are affected only by inevitable numerical errors, which are, in all cases, many orders of magnitude lower than any experimental error. Therefore, if the same data were obtained from an experimental analysis, the effective significance of their maximum point as the value where the optimum n is found would be questionable since the experimental errors could cover the little difference in the values of R^2. In this analysis, the difference in the R^2 value (5×10^{-4}) is very high with respect to the numerical errors of the computer calculations (~10^{-15}), and hence, the maximum R^2 surely identifies the optimum value of n for this step. These considerations are general and, thus, hold also for the analysis of the other permeation steps studied. Considering the curves at different temperatures, it is possible to notice the remarkable dependence of the system behavior on temperature. In particular, for the lowest temperature considered (270 °C), a maximum value of R^2 that is located in correspondence of an n of about 0.582 is found, as also reported in Table 3. As the temperature increases, this value progressively decreases down to a value of 0.539 at 500 °C. As also discussed previously, this behavior is explained by considering the role of the term b, which includes the interactions among the hydrogen atoms in the metal bulk. Let us recall that in this study, the Young modulus Y_S and the hydrogen partial molar volume $\bar{V}_H$ in the lattice were considered as constants because of the low value of the hydrogen content in the Pd bulk (~0.03). In fact, in eq 7, the term involving b decreases with temperature, and hence, according to this model, the system tends to the perfect Sieverts-type behavior at a high temperature.

Naturally, these particular numerical values of n are strictly related to this particular membrane since another membrane could have been subjected to other thermal/mechanical conditions during

TABLE 3: Optimal Sieverts Exponent for Diffusion-Limited Permeation at Several Temperatures

Diffusion-Limited Permeation		
	optimal n	
temperature	calculated from the data of Peters et al.[10]	calculated from the data of Barbieri et al.[16]
270 °C	0.582	0.506
300 °C	0.573	0.505
350 °C	0.562	0.503
400 °C	0.552	0.502
450 °C	0.545	0.501
500 °C	0.539	0.500

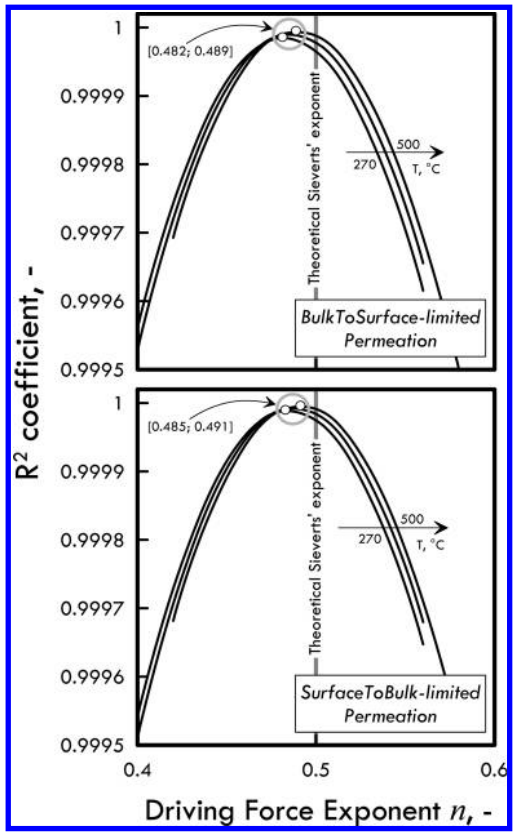

Figure 5. R^2 regression coefficient as a function of the driving force exponent in the case of surface-to-bulk- and bulk-to-surface-limited permeation for different temperatures.

its preparation or use. Sometimes, when from permeation tests a driving force exponent not so different from 0.5 is found, it is still usual to adopt 0.5 in the permeation law. In this case, it can be useful to change the temperature and check if the n value has been significantly changed. If this second condition occurs, probably the nonlinear behavior of the diffusion in the lattice is playing an appreciable role in the permeation. Analyzing Figure 4b corresponding to the other diffusional parameters (data from ref 16), a quite different situation is found. In fact, all of the curves are very close to each other and reach a maximum of R^2 in correspondence of an n value of 0.5. Therefore, if summarizing the results shown in Figure 4, it is possible to say that the model foresees an n exponent that varies from ~0.5 to 0.6 in dependence of the membrane considered. If the same kind of analysis is carried out for the transition steps surface-to-bulk and bulk-to-surface, the results shown in Figure 5 are obtained, with the optimal n values staying in the range of 0.48−0.49 and not depending on temperature.

The first thing to notice is that here, there is no appreciable influence of the different diffusional parameters calculated and used

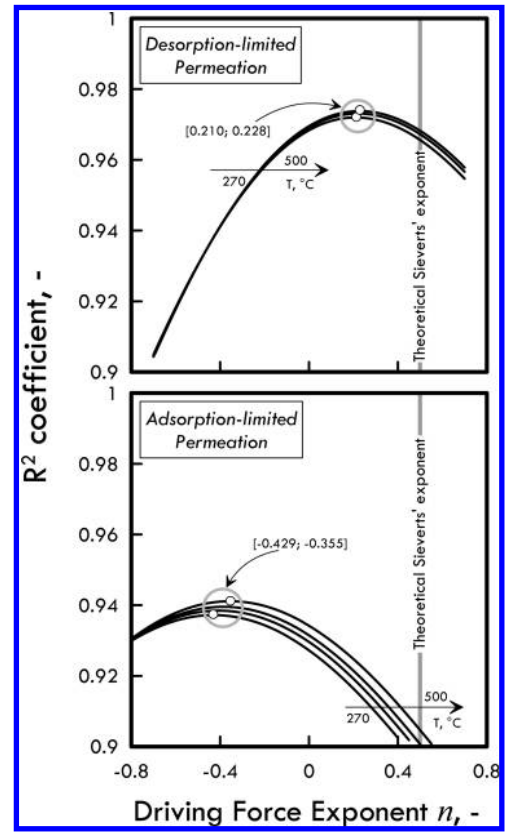

Figure 6. R^2 regression coefficient as a function of the driving force exponent in the case of adsorption- and desorption-limited permeation for different temperatures.

in the simulation. Moreover, the two steps present the analogous qualitative behavior, and the curves are very similar even from a quantitative point of view. The fact that the maximum values for R^2 are very close to the unitary value indicates the level of goodness in adopting a Sieverts-type driving force for the step(s) considered. The similarity of the optimal n to the value of 0.5 indicates that the original Sieverts law can be valid also for these steps. This confirms the validity of the hypotheses used to achieve eq 6, which foresees a driving force expressible in terms of the pressure square-root difference in the case of $\theta \approx 1$ and $\xi \ll 1$. However, the complexity of the theoretical model considered does not always allow, in principle, a simple form for the permeation driving force to be achieved. This consideration is not trivial since actually it is not true that, in general, the characteristic driving force of a permeation step can be well-represented by a Sieverts-type expression.

This fact can be shown more clearly if the steps of adsorption and desorption (Figure 6) are analyzed analogously to what was done for the previous steps. Let us recall that the two cases refer to a situation in which each step was considered singularly as the limiting one. In this case, a very different situation can be observed. First of all, the diffusional parameters do not influence these steps since the diffusion step is considered at the equilibrium. However, the most important result shown in this figure is that for both adsorption and desorption, the maximum values of R^2 at different temperatures are significantly lower than the ones found for diffusion and the two transitions, especially as concerns the adsorption step. Examining first this last one, for all of the temperatures considered, the maxima reach more or less 0.94, in correspondence of which n values staying in the range of $[-0.429, -0.355]$ are found.

Analogous results are achieved for the desorption step, which, however, shows quite different values for n and R^2 with respect

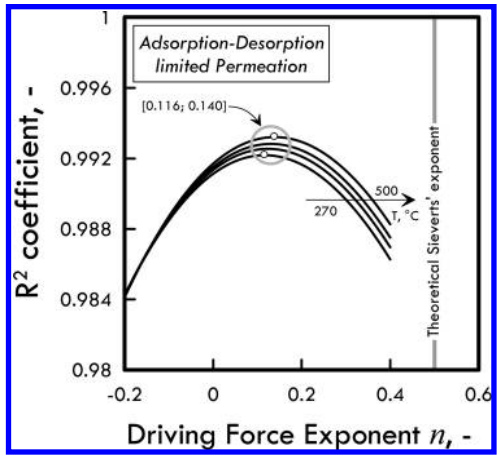

Figure 7. R^2 regression coefficient as a function of the driving force exponent in the case of both surface phenomena-limited permeation for different temperatures.

to the ones of the adsorption. In this case, the n values are positive, and the R^2 values are ~0.975 higher than those related to the adsorption but still too lower than 1. This means that, in general, it is not possible to describe the permeation driving force of both adsorption and desorption by means of a Sieverts-type expression without making a significant error that could alter the interpretation of the experimental results. In other words, the quite low values of R^2 indicate that there no n exponents exist for which the driving forces reported in eqs 4 and 8 are well-approximated.

However, adsorption and desorption usually provide influences that are comparable to each other, as will be shown later the paper (Figure 10). Therefore, it can be interesting to analyze the system behavior when both of the surface phenomena are the limiting steps at the same time (as usual, in this analysis, the other steps will be considered at the equilibrium). The results of this kind of investigation are shown in Figure 7, where the optimal exponent n is evaluated by finding for each temperature the maximum regression coefficient of the surface phenomena-limited flux versus a Sieverts-type driving force. The main difference that is possible to observe in this plot with respect to the case in which adsorption and desorption were considered separately is that here, the maximum R^2 coefficient is quite higher than before (>~0.992). This means that, different from what was seen for the individual cases of adsorption- and desorption-limited permeation, the adsorption−desorption-limited permeation is characterized by a driving force that can be represented with a good approximation by a Sieverts-type expression.

The overall comparison concerning the surface phenomena is reported in Table 4, where, for each case, both the Sieverts-type driving force and those evaluated in the previous sections

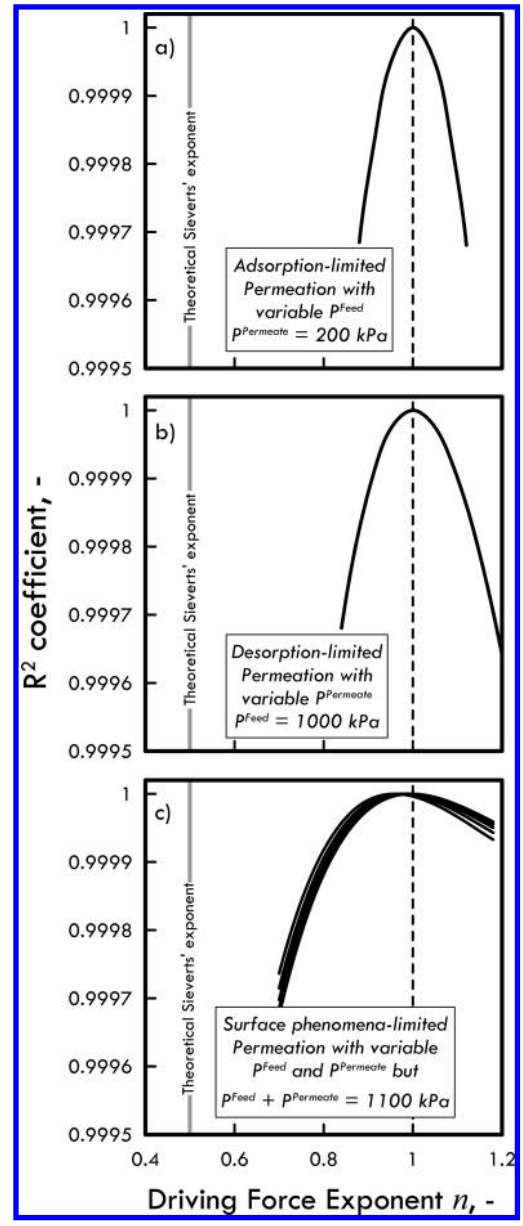

Figure 8. R^2 regression coefficient as a function of the driving force exponent in the case of (a) adsorption-limited permeation with constant permeate pressure, (b) desorption-limited permeation with constant feed pressure, and (c) adsorption−desorption-limited permeation with a constant sum of feed and permeate pressures at different temperatures.

are shown with the respective values of exponent n and R^2. At this point, it is necessary to emphasize that in this investigation, the driving force is determined by varying both the feed and

TABLE 4: Permeation Driving Forces, Sieverts Exponent, and Corresponding R^2 for Adsorption-, Desorption-, and Both Surface Phenomena-Limited Permeation

step-limited permeation			
limiting steps	permeation driving force	n	maximum R^2 (@ 270 °C)
adsorption	$P^F_{H_2} - P^P_{H_2} \Big/ P^P_{H_2} = \phi - 1$	1, with $P^P_{H_2}$ constant	0.9998
	$[(P^F_{H_2})^{n_1} - (P^P_{H_2})^{n_1}]$	[−0.429; −0.355]	0.9374
desorption	$(P^F_{H_2} - P^P_{H_2}) \Big/ P^F_{H_2} = (\phi - 1)/\phi$	1, with $P^F_{H_2}$ constant	0.9997
	$[(P^F_{H_2})^{n_2} - (P^P_{H_2})^{n_2}]$	[0.210; 0.228]	0.9721
both surface phenomena at the same time	$(P^F_{H_2} - P^P_{H_2}) \Big/ (P^F_{H_2} + P^P_{H_2}) = (\phi - 1)/(\phi + 1)$	[0.97; 1], with $P^F_{H_2} + P^P_{H_2}$ constant	1.0000
	$[(P^F_{H_2})^{n_3} - (P^P_{H_2})^{n_3}]$	[0.116; 0.140]	0.9924

TABLE 5: Permeation Driving Forces with the Corresponding Values of n and R^2 for Each Limiting Step

	step-limited permeation		
permeation steps	permeation driving force	n	lowest maximum R^2
surface-to-bulk and bulk-to-surface	$[(P^F_{H_2})^{n_1} - (P^P_{H_2})^{n_1}]$	[0.485; 0.492]	1.00000
diffusion	$[(P^F_{H_2})^{n_2} - (P^P_{H_2})^{n_2}]$	[0.500; 0.585]	1.00000
both surface phenomena	$(P^F_{H_2} - P^P_{H_2}) / (P^F_{H_2} + P^P_{H_2}) = (\phi - 1)/(\phi + 1)$	[0.97; 1], with $P^F_{H_2} + P^P_{H_2}$ constant	1.00000
	$[(P^F_{H_2})^{n_3} - (P^P_{H_2})^{n_3}]$	[0.116; 0.140]	0.9924

permeate pressures independently of each other in order to be sure that the driving force is the most general that is possible and does not depend on the particular single values of the pressures considered. As regards the theoretical n value, as also mentioned in the previous section, it is possible to express the various driving forces in the form of a Sieverts-type expression only in particular cases, which depend on the particular operating conditions considered. In particular, regarding the adsorption step, if the pressure of the permeate is set to be constant, the driving force is reduced to the simple difference between the feed and permeate pressures since the denominator in eq 4 becomes constant. Therefore, the value of the exponent n must be equal to 1 for all of the temperatures considered. Analogously, regarding the desorption step, if the feed pressure is set to be constant, for the same reasons, the permeation driving force becomes the simple difference of the feed and permeate sides, and thus, n is 1 also (see eq 8).

Similar results are obtained if both surface phenomena are the rate-determining steps and the feed and permeate pressures are chosen in such a way that their sum is constant, causing the driving force introduced in eq 9 to be the simple pressure difference. Furthermore, if in this case the permeate pressure is chosen to be very low with respect to the feed one, the driving force tends to be very close to the unitary value for every feed pressure. Therefore, under these conditions, the flux would be virtually dependent only on the temperature, and its maximum value could be reached by each driving force fulfilling the above-mentioned hypothesis of very low permeate pressure.

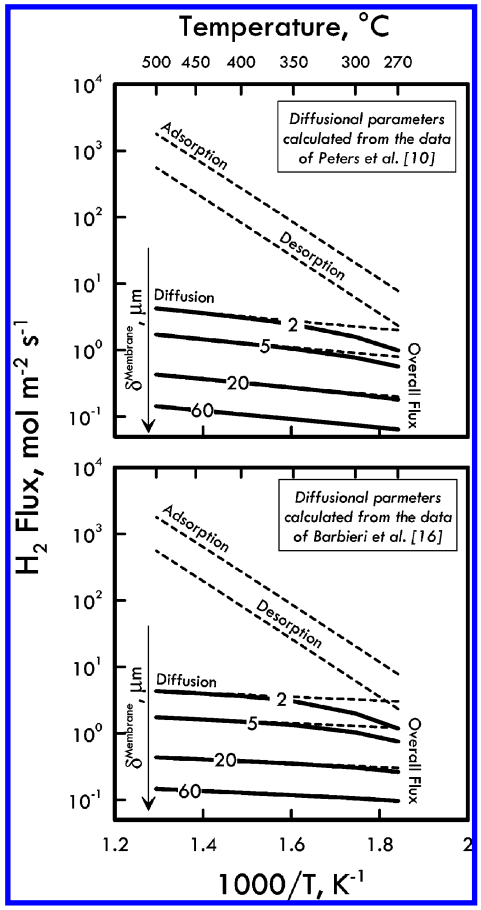

Figure 9. Rate-limited fluxes (dashed line) and overall flux (solid line) as functions of temperature for different membrane thicknesses; P_F = 1000 kPa, P_P = 300 kPa.

These important results are shown in Figure 8, where (a) a constant permeate pressure of 200 kPa was considered for the adsorption step, (b) a constant feed pressure of 1000 kPa was considered for the desorption step, and (c) a constant sum of feed and permeate pressures of 1100 kPa was considered for the adsorption−desorption at the same time. Further quantitative evidence of the system behavior is provided in the summarizing Table 5, which reports the driving force and the corresponding value of the maximum R^2 for each limiting step. Concerning the adsorption and desorption steps, only the case of both surface phenomena-limited permeation was reported in the table since, actually, this is a more significant case with respect to the one when each of them is considered individually as the rate-determining step because the rates of adsorption and desorption are usually comparable to each other.

In Figure 9, the rate-limited fluxes (dashed lines) and the overall resulting fluxes (continuous line) are reported as a function of temperature for different membrane thicknesses. The qualitative behavior of the two systems considered is the same, even though the one related to the work of Peters et al.[10] is a little bit more sloped than the other one. In these plots, the curves of adsorption- and desorption-limited fluxes are the same in both cases since these two steps are not dependent on the different diffusional parameters, whereas the diffusion-limited curves depend on them. Furthermore, they present a slope quite higher than the one of the diffusion, this characterizing a typical behavior of the kinetic phenomenon than is generally faster than a diffusional one.

The transitions surface-to-bulk and bulk-to-surface do not provide any appreciable influence in these conditions and, therefore, are not reported in figure. Analyzing the plots, for low membrane thicknesses (2, 5 μm), at low temperature, the overall fluxes significantly differ from the diffusion-limited behavior, while at high temperature, they follow the diffusion curves (diffusion-controlled systems). For higher membrane thicknesses, the systems follow the diffusion-limited fluxes even at low temperature. This means that there is a certain range of conditions where the surface phenomena provide a significant influence on the permeation process. This influence can be better observed for both systems by looking at Figure 10, where it is expressed quantitatively under the same conditions as the ones considered in the previous figure.

The way of evaluating the influence of each step is related to the ratio of the limiting fluxes, whose details are reported in Appendix B. In this figure, considering the 2 μm case, which is just the membrane considered by Peters et al.[10] in their work

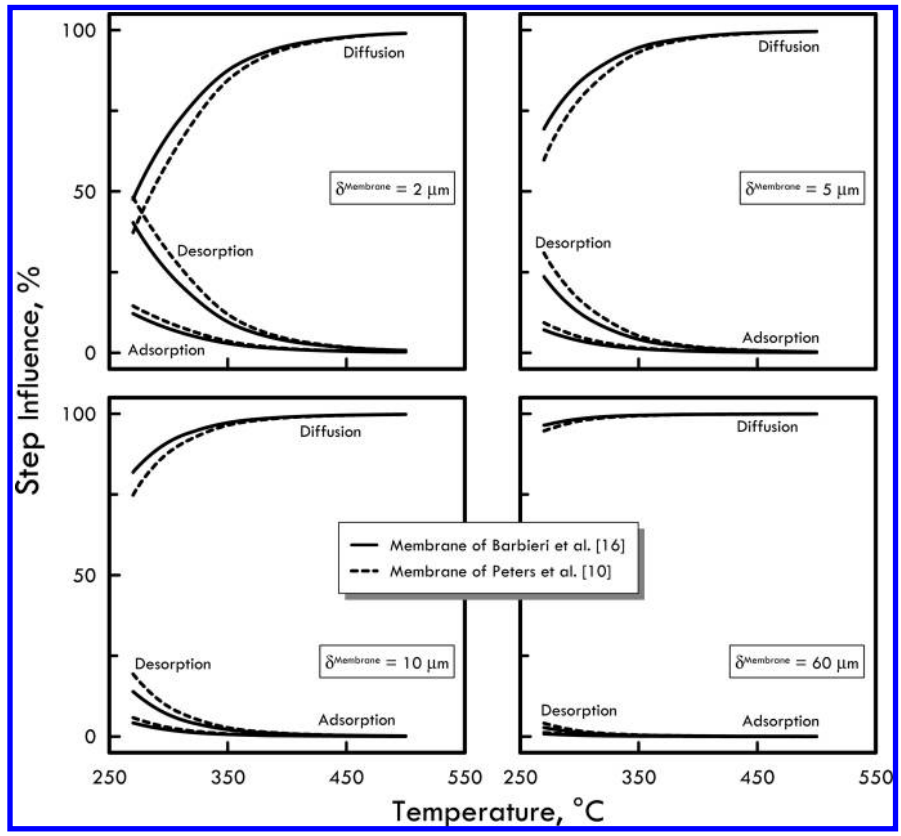

Figure 10. Influence of the main permeation steps as a function of temperature for different membrane thicknesses. The nonreported steps do not provide any significant influence. $P_F = 1000$ kPa, $P_P = 300$ kPa.

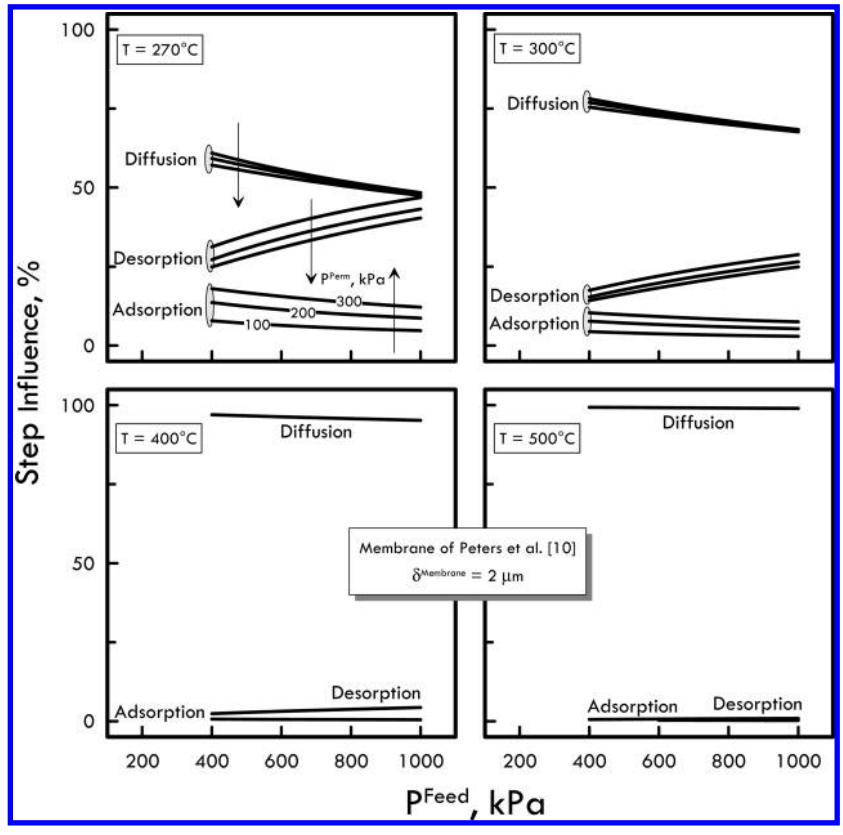

Figure 11. Influence of the main permeation steps as a function of feed pressure for different permeate pressures and temperatures calculated for Peters et al.[10] system ($\delta^{Mem} = 2$ μm). The order of the permeate pressures in all of the plots is the same as the one indicated by the arrow and the numerical values at 270 °C.

(dashed lines), surface phenomena and diffusion provide overall influences of about 52 and 48%, respectively, at 270 °C. As the temperature increases, the influence of adsorption and desorption decreases quite rapidly due to the fact that their specific rates become progressively faster than the ones of the diffusion, which is characterized by a lower activation energy. An analogous qualitative behavior can be observed for the other thicknesses, at which, however, the influence of the surface phenomena is appreciable only at temperature lower than 350 °C up to 10 μm, becoming negligible for thicker membranes (>60 μm). The difference between the two systems considered is due to the fact that the diffusional parameters calculated for the membrane of Barbieri et al.[16] allow the atomic hydrogen to diffuse through the metal lattice with more facility than the other one. By analyzing the effect of the other operating conditions (feed and permeate pressures) on the influence of the main permeation steps (Figure 11), several aspects can be found. In this figure, only the membrane of Peters et al.[10] is considered because it presents analogous behavior with respect to the other one. Considering the case at 270 °C, the diffusion and adsorption influences decrease with the feed pressure, whereas the one of the desorption shows the opposite behavior. This occurs because the forward adsorption rate is proportional to the feed pressure, which causes this step to be faster. The opposite case occurs for the desorption rate, which is not favored by an increasing feed pressure. Concerning the diffusion, it becomes more rapid as the feed pressure increases, causing the increase of the desorption influence to be a little bit more significant with respect to the adsorption decrease.

Regarding the effect of the permeate pressure, this one affects more the adsorption rate than the desorption one for the analogous reasons already explained for the feed pressure effect, whereas the diffusion step is shown to be not very affected by a change of permeate pressure. At this point, all of these considerations have to be finalized toward the investigation on the main topic of this paper, that is, how all of these effects affect the values of the exponent n.

In Figure 12, the overall Sieverts driving force exponent is reported as a function of temperature for both systems considered. According to the different diffusional parameters, the curves show a nonmonotonic (membrane of Peters et al.[10]) or monotonic (membrane of Barbieri et al.[16]) behavior (except for 60 μm, where there is a maximum at about 370 °C). In particular, in the first case, the curves present a maximum for membrane thickness lower than 20 μm, whereas the one at 60 μm is continuously decreasing toward the value of 0.5. On the contrary, in the second case, the n exponent increases with temperature, approaching the value of 0.5. As it is possible to see, at a low temperature, where it has been previously shown that the surface phenomena provide a significant contribution, the value of n is quite lower than the theoretical value of 0.5 (classical Sieverts law exponent) in both cases.

This situation is dually represented if the n exponent is reported as a function of the membrane thickness (Figure 13), which is the other factor that directly influences the effect of the hydrogen diffusion in the Pd-based layer. From this plot, an important aspect to be highlighted is that the same material (from the diffusional parameters point of view) at the same temperature (<350 °C in the considered cases) can provide a nonconstant driving force exponent. This is due to the increasing influence of the diffusion, whose characteristic flux depends on the membrane thickness with an inverse proportionality. At high temperature (>~400 °C), where the diffusion tends to be the unique limiting step, the membrane thickness does not provide any influence on the n exponent, whose value depends on the particular diffusional characteristics of the membrane (~0.5 for the membrane of Barbieri et al.[16] and ~0.53 for the membrane of Peters et al.[10]).

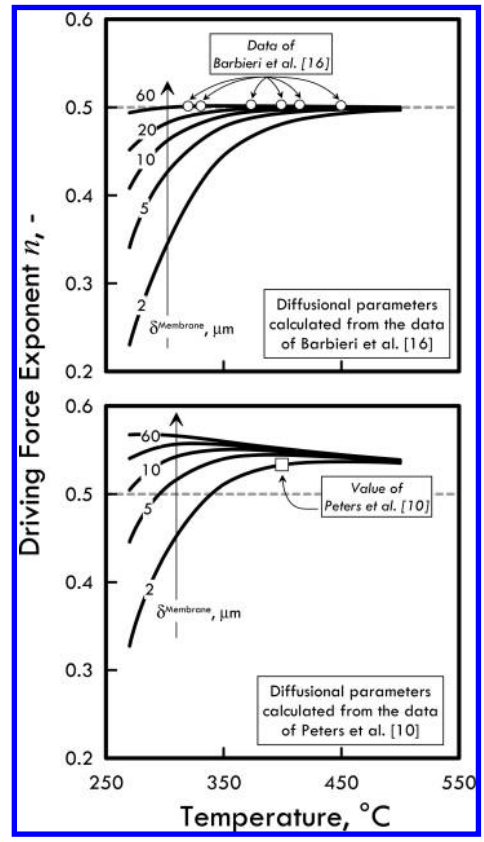

Figure 12. Driving force exponent as a function of temperature for different membrane thicknesses.

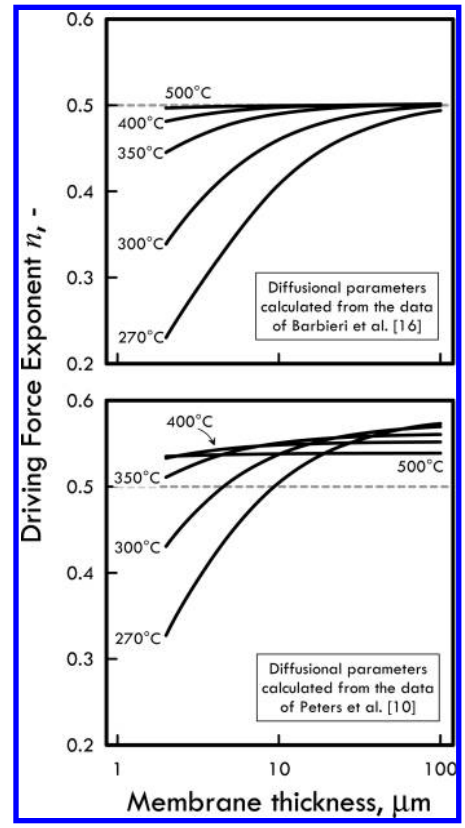

Figure 13. Driving force exponent as a function of membrane thickness for different temperatures.

5. Conclusions

In this work, an investigation on the theoretical meaning of the Sieverts exponent n was performed by means of a complex model that divides the overall hydrogen permeation into several elementary steps. The driving force corresponding to each of these steps (adsorption, desorption, diffusion in the Pd-based layer, and the two transitions surface-to-bulk and bulk-to-surface) was evaluated, identifying in this way for each of them also the related exponent n. It was shown that, in general, the adsorption and desorption singularly considered are not well-described by a Sieverts-type driving force, they being characterized by driving forces depending on the ratio of the feed and permeate hydrogen pressures. When adsorption and desorption are considered at the same time, they are better modeled by a Sieverts-type relation, presenting, in general, a value of n close to 0.2. However, it is shown that under particular operating conditions (at a constant sum of the hydrogen pressures), the theoretical value of n is 1, even when adsorption and desorption are considered separately (at constant feed or permeate hydrogen pressures, respectively). Concerning the diffusion, a permeation driving force was found that can be divided into two contributions, one which is the original Sieverts law ($n = 0.5$) and the other which coincides with the simple difference of the hydrogen partial pressures ($n = 1$). This expression provides a theoretical explanation for the reason why some very thick membranes show a Sieverts exponent higher than 0.5. Then, the model was numerically solved for two membranes taken from some works in the literature,[10,16] for which the respective diffusional parameters were evaluated. In this way, the n exponent associated with each permeation step and the overall was achieved as a function of the operating conditions (temperature, membrane thickness, and hydrogen pressures on the feed and permeate sides). It was shown that at a low temperature and thin membrane thickness, a decrease of the overall exponent n occurs toward values lower than 0.5. At a higher temperature and thickness (diffusion-controlled permeation), the membranes show n values tending to 0.5 with different rapidity according to the different diffusional parameters calculated.

Appendix A: Evaluation of the Step-Limited Permeation Laws

In this appendix, there are details of how the permeation law of each step-limited flux is achieved. To do that, in the first subsection, the flux related to each step will be recalled, in the second one, the equilibrium relations for each steps will be achieved, and finally, in the third one, the step-limited fluxes will be obtained by coupling the relations of the previous sections. In the following relations, the notation of the variable subscripts is found in Figure 1. The numerical values of the parameters used in the simulation are reported in Table A1.

A1. Permeation Step Fluxes. *A1.1. Adsorption and Desorption.* The flux of the adsorption and desorption step has already been described and used in some previous works in the literature[2,3,18,19] (eqs 10, 11).

$$J_{H_2}^{Ads} = \frac{S_0 F(\theta_F)}{\sqrt{2\pi M_{H_2} RT}} P_F - N_s^2 k_{Des}^0 \exp\left(-\frac{2E_{Des}}{RT}\right)\theta_F G(\theta_F) \tag{10}$$

$$J_{H_2}^{Des} = N_s^2 k_{Des}^0 \exp\left(-\frac{2E_{Des}}{RT}\right)\theta_P G(\theta_P) - \frac{S_0 F(\theta_P)}{\sqrt{2\pi M_{H_2} RT}} P_P \tag{11}$$

The functionalities hidden and collected in the terms $F(\theta)$ and $G(\theta)$ are described in eqs 12−15, where the limit case of θ tending to 1 is also indicated because in the body of the present paper is explained that this situation is very close to the numerical solution of all of the coupled equations considered.

$$F(\theta) = \frac{1}{\left[1 + K\left(\frac{1}{(1-\theta) - H(\theta)} - 1\right)\right]}$$
$$F(\theta \to 0) = \frac{1}{(1 + 2K\theta)} \qquad F(\theta \to 1) = \frac{(1-\theta)^2}{K} \tag{12}$$

TABLE A1: Values of the Parameters and Physical Constants Used in the Simulation

c_1, $m^{0.5}\ K^{0.5}\ s\ kg^{-0.5} =$	10.154	E_{BS}, J $mol^{-1} =$	E_{Diff}
E_{SB}, J $mol^{-1} =$	$E_{BS} + 0.5(\Delta E_{Ads} - \Delta E_{Abs})$	E_{Des}, J $mol^{-1} =$	$0.5\Delta E_{Abs}$
$K =$	0.05	N_b, $mol_{Pd}\ m^{-3} =$	1.13×10^5
N_s, $mol_{Pd}\ m^{-2} =$	2.8×10^{-5}	$S_0 =$	1
ΔE_{Abs}, J $mol_H^{-1} =$	16 736	ΔE_{Ads}, J $mol_H^{-1} =$	83 680
k^0_{Des}, $m^2\ s^{-1}\ mol^{-1} =$	4.8×10^{17}	λ_{j0}, $s^{-1} =$	2.30×10^{13}
ω, J $mol^{-1} =$	2092	ΔE_{SB}, J $mol_H^{-1} =$	$E_{SB} - E_{BS}$

TABLE A2: Equilibrium Relations for Each Permeation Step

steps involved in	expression	
adsorption and desorption	$\frac{S_0}{K\sqrt{2\pi M_{H_2} RT}}(1-\theta)^2 P = N_s^2 k_{Des}^0 \exp\left(-\frac{2E_{Des}}{RT}\right)\theta^2$	(26)
surface-to-bulk and bulk-to-surface	$(1-\xi)\frac{T^{0.25}}{c_1}\exp\left(-\frac{\Delta E_{SB}}{RT}\right)\sqrt{K}\frac{\theta}{1-\theta} = \xi$ $\Delta E_{SB} \equiv E_{SB} - E_{BS}$	(27)
diffusion	$(\xi_F - \xi_P) + \left(\frac{1}{2} + \frac{b}{T}\right)(\xi_F^2 - \xi_P^2) = 0 \Rightarrow \xi_F = \xi_P$	(28)

$$G(\theta) = \frac{1}{\theta}[\theta - \mathrm{H}(\theta)], \qquad G(\theta \to 0) = 0 \qquad G(\theta \to 1) = \theta \tag{13}$$

$$H(\theta) = \left[\frac{2\theta(1-\theta)}{\mathrm{Den}(\theta)}\right], \qquad H(\theta \to 0) = \theta \qquad H(\theta \to 1) = \theta(1-\theta) \tag{14}$$

$$\mathrm{Den}(\theta) = 1 + \sqrt{1 - 4\theta(1-\theta)\left[1 - \exp\left(\frac{\omega}{RT}\right)\right]} \qquad \mathrm{Den}(\theta \to 0) = 2 \qquad \mathrm{Den}(\theta \to 1) = 2 \tag{15}$$

Substituting eqs 12−15 into eq 10 under the hypothesis of $\theta \approx 1$, eqs 16 and 17 are obtained, which are very good approximations of eqs 10 and 11, respectively, under the conditions considered in the present paper.

$$J_{\mathrm{H_2}}^{\mathrm{Ads}} \cong \frac{S_0}{K\sqrt{2\pi M_{\mathrm{H_2}} RT}}(1-\theta_{\mathrm{F}})^2 P_{\mathrm{F}} - N_{\mathrm{s}}^2 k_{\mathrm{Des}}^0 \exp\left(-\frac{2E_{\mathrm{Des}}}{RT}\right)\theta_{\mathrm{F}}^2 \tag{16}$$

$$J_{\mathrm{H_2}}^{\mathrm{Des}} \cong N_{\mathrm{s}}^2 k_{\mathrm{Des}}^0 \exp\left(-\frac{2E_{\mathrm{Des}}}{RT}\right)\theta_{\mathrm{P}}^2 - \frac{S_0}{K\sqrt{2\pi M_{\mathrm{H_2}} RT}}(1-\theta_{\mathrm{P}})^2 P_{\mathrm{P}} \tag{17}$$

A1.2. Surface-to-Bulk and Bulk-to-Surface. The relations used to model these two transitions steps (eqs 18 and 19) were developed by Ward and Dao[2] in their paper and used also by Caravella et al.[3] in their extended model.

$$J_{\mathrm{H_2}}^{\mathrm{SB}} = \frac{N_{\mathrm{s}}\lambda_{\mathrm{j0}}}{6}\left[(1-\xi_{\mathrm{F}})\frac{T^{0.25}}{c_1}\exp\left(-\frac{E_{\mathrm{SB}}}{RT}\right)\sqrt{\frac{G(\theta_{\mathrm{F}})\theta_{\mathrm{F}}}{F(\theta_{\mathrm{F}})}} - \xi_{\mathrm{F}}\exp\left(-\frac{E_{\mathrm{BS}}}{RT}\right)\right] \tag{18}$$

$$J_{\mathrm{H_2}}^{\mathrm{BS}} = \frac{N_{\mathrm{s}}\lambda_{\mathrm{j0}}}{6}\left[\xi_{\mathrm{P}}\exp\left(-\frac{E_{\mathrm{BS}}}{RT}\right) - (1-\xi_{\mathrm{P}})\frac{T^{0.25}}{c_1}\exp\left(-\frac{E_{\mathrm{SB}}}{RT}\right)\sqrt{\frac{G(\theta_{\mathrm{P}})\theta_{\mathrm{P}}}{F(\theta_{\mathrm{P}})}}\right] \tag{19}$$

Using the usual hypothesis of θ close to 1, eqs 20 and 21 are achieved

$$J_{\mathrm{H_2}}^{\mathrm{SB}} \cong \frac{N_{\mathrm{s}}\lambda_{\mathrm{j0}}}{6}\left[(1-\xi_{\mathrm{F}})\frac{T^{0.25}}{c_1}\exp\left(-\frac{E_{\mathrm{SB}}}{RT}\right)\sqrt{K}\frac{\theta_{\mathrm{F}}}{1-\theta_{\mathrm{F}}} - \xi_{\mathrm{F}}\exp\left(-\frac{E_{\mathrm{BS}}}{RT}\right)\right] \tag{20}$$

$$J_{\mathrm{H_2}}^{\mathrm{BS}} \cong \frac{N_{\mathrm{s}}\lambda_{\mathrm{j0}}}{6}\left[\xi_{\mathrm{P}}\exp\left(-\frac{E_{\mathrm{SB}}}{RT}\right) - (1-\xi_{\mathrm{P}})\frac{T^{0.25}}{c_1}\exp\left(-\frac{E_{\mathrm{SB}}}{RT}\right)\sqrt{K}\frac{\theta_{\mathrm{P}}}{1-\theta_{\mathrm{P}}}\right] \tag{21}$$

A1.3. Diffusion. The equations used to model the diffusion of atomic hydrogen through the Pd-based lattice in the present paper (eqs 22−24) were developed by Caravella et al.,[3] who considered the gradient of the hydrogen chemical potential as the driving force of the permeating flux.

$$J_{\mathrm{H_2}}^{\mathrm{Diff}} = \frac{N_{\mathrm{b}}}{2\delta^{\mathrm{Mem}}}D_{\mathrm{H}}^0\exp\left(-\frac{E_{\mathrm{Diff}}}{RT}\right)\left[\ln\left(\frac{1-\xi_{\mathrm{P}}}{1-\xi_{\mathrm{F}}}\right) + \frac{b}{T}(\xi_{\mathrm{F}}^2 - \xi_{\mathrm{P}}^2)\right] \tag{22}$$

$$b = \frac{w_{\mathrm{HH}} + \frac{1}{3}N_{\mathrm{b}}Y_{\mathrm{S}}\bar{V}_{\mathrm{H}}^2}{2R} \tag{23}$$

If the logarithmic term is developed in Mac Lauren's series (around $\xi = 0$) and an approximation of the second order is used, eq 25 is valid. The second-order approximation allows very good accuracy in the range of values of ξ, which does not exceed the value of 0.06 in the operating conditions considered in the present paper.

$$\ln(1-\xi) = -\xi - \frac{\xi^2}{2} + o(\xi^3) \qquad \ln\left(\frac{1-\xi_{\mathrm{P}}}{1-\xi_{\mathrm{F}}}\right) \cong (\xi_{\mathrm{F}} - \xi_{\mathrm{P}}) + \frac{(\xi_{\mathrm{F}}^2 - \xi_{\mathrm{P}}^2)}{2} \tag{24}$$

Substituting eq 25 into eq 22, eq 23 is obtained. In the next sections, the variables ξ will be expressed as functions of the hydrogen pressures to find the characteristic driving force of the diffusion flux.

$$J_{\mathrm{H_2}}^{\mathrm{Diff}} = \frac{N_{\mathrm{b}}}{2\delta^{\mathrm{Mem}}}D_{\mathrm{H}}^0\exp\left(-\frac{E_{\mathrm{Diff}}}{RT}\right)\left[(\xi_{\mathrm{F}} - \xi_{\mathrm{P}}) + \left(\frac{1}{2} + \frac{b}{T}\right)(\xi_{\mathrm{F}}^2 - \xi_{\mathrm{P}}^2)\right] \tag{25}$$

A2. Equilibrium Relations. The equilibrium relations are achieved by setting the equality between the forward and reverse rate for each step. In the following expressions (Table A2), there are no subscripts indicating the side on which the variables are considered since at the equilibrium, the same equalities can be applied on both membrane sides according to the particular step to be examined.

A3. Step-Limited Fluxes. To achieve the step-limited permeation laws, the flux of each step has to be combined with the equilibrium relations of the other steps. The final aim of this section is to express the variables θ and ξ, which are nondirectly evaluated, as functions of the hydrogen pressures P in order to recognize the driving force of the step considered. In the following subsections, the subscript Lim will be used to indicate the step-limited fluxes and distinguish them from the true fluxes expressed by eqs 10−17.

A3.1. Adsorption-Limited Permeation. To obtain the permeation law for the adsorption step, we have to express the variable

θ_F in eq 16 in terms of the hydrogen pressure on the permeate side P_P. To do that, let us combine the equilibrium relations reported in Table A2. The overall result of this combination is eq 29, where it is shown that the two surface coverages θ_F and θ_P are equal.

$$\theta_F = \theta_P, \Rightarrow (1 - \theta_F)^2 = (1 - \theta_P)^2 \cong \frac{1}{P_P}\frac{N_s^2 k_{Des}^0}{S_0}\exp\left(-\frac{2E_{Des}}{RT}\right)K\sqrt{2\pi M_{H_2} RT}\Big|_{\theta\cong 1} \quad (29)$$

If eq 29 is used in eq 16, the following expression for the adsorption-limited flux is obtained (eq 30), where the parameter ϕ has been already defined in eq 5

$$J_{H_2,Lim}^{Ads} = \pi_{H_2}^{Ads}(T)\left(\frac{P_F - P_P}{P_P}\right) = \pi_{H_2}^{Ads}(T)(\phi - 1)$$
$$\pi_{H_2}^{Ads}(T) \equiv N_s^2 k_{Des}^0 \exp\left(-\frac{2E_{Des}}{RT}\right) \quad (30)$$

A3.2. Surface-to-Bulk-Limited Permeation. In this case, the target equation to be considered is eq 20, where the variables θ_F and ξ_F have to be expressed in terms of P_F and P_P, respectively. Therefore, by manipulating the equilibrium relations in Table A2, eqs 31 and 32 are achieved, which can be substituted in eq 20 obtaining in this way the flux as a function of only the feed and permeate hydrogen pressures (eq 33).

$$\left(\frac{S_0}{N_s^2 k_{Des}^0 \exp\left(-\frac{2E_{Des}}{RT}\right)K\sqrt{2\pi M_{H_2} RT}}\right)^{0.5} P_F^{0.5} = \left(\frac{\theta_F}{1 - \theta_F}\right) \quad (31)$$

$$\xi \ll 1 \Rightarrow \xi_F = \xi_P \cong \frac{\exp\left(\frac{E_{Des} - \Delta E_{SB}}{RT}\right)S_0^{0.5}}{c_1 N_s (k_{Des}^0)^{0.5}(2\pi M_{H_2} R)^{0.25}} P_P^{0.5} \quad (32)$$

$$J_{H_2,Lim}^{SB} \cong \pi_{H_2}^{SB}(T)[P_F^{0.5} - P_P^{0.5}]$$
$$\pi_{H_2}^{SB}(T) \equiv \frac{\lambda_{j0} S_0^{0.5} \exp\left(\frac{E_{Des} - E_{SB}}{RT}\right)}{6c_1 (k_{Des}^0)^{0.5}(2\pi M_{H_2} R)^{0.25}} \quad (33)$$

It is possible to notice that this flux corresponds to the original Sieverts-type expression ($n = 0.5$).

A3.3. Bulk-to-Surface-Limited Permeation. Applying the analogous procedure as the one performed for the surface-to-bulk case, exactly the same expression as eq 33 is found. Therefore, both of the transition phenomena can be expressed by a Sieverts law relation in the hypotheses of $\theta \rightarrow 1$ and $\xi \ll 1$.

A3.4. Diffusion-Limited Permeation. The diffusion-limited permeation certainly represents the most important case among the here-considered ones because it is the closest condition to a real one. In this case, the atomic hydrogen concentrations ξ_F and ξ_P in eq 25 have to be expresses in terms of the hydrogen pressure of the feed (P_F) and permeate sides (P_P), respectively. Due to the position of the diffusion step according to the flux direction, the procedure to express ξ_F as a function of P_F brings the same results as the one obtained for the other side of the membrane. Therefore, only the first case will be shown. If the equilibrium relations reported in Table A2 are combined with each other for the feed side, eq 34 is obtained.

$$\frac{\exp\left(\frac{E_{Des} - \Delta E_{SB}}{RT}\right)S_0^{0.5}}{c_1 N_s (k_{Des}^0)^{0.5}(2\pi M_{H_2} R)^{0.25}} P_F^{0.5} = \frac{\xi_F}{(1 - \xi_F)} \quad (34)$$

Exploiting the hypothesis of $\xi_F \ll 1$ and collecting the functionality with temperature in the term $a(T)$, eqs 35 and 36 are achieved.

$$\xi_F \ll 1 \Rightarrow \xi_F \cong a(T) P_F^{0.5} \quad (35)$$

$$a(T) \equiv a_0 \exp\left(\frac{\Delta E_{Ab}}{2RT}\right)$$
$$a_0 \equiv \frac{S_0^{0.5}}{c_1 N_s (k_{Des}^0)^{0.5}(2\pi M_{H_2} R)^{0.25}}$$
$$\Delta E_{Ab} \equiv 2(E_{Des} - \Delta E_{SB}) \quad (36)$$

Substituting eq 35 in eq 25 and applying the same procedure for the permeate side, the diffusion-limited flux is expressed as a function of the two hydrogen pressures (eq 37).

$$J_{H_2,Lim}^{Diff} = \pi_{H_2}^{Diff}(T, \delta^{Mem})\left[(P_F^{0.5} - P_P^{0.5}) + a(T)\left(\frac{1}{2} + \frac{b}{T}\right)(P_F - P_P)\right]$$
$$\pi_{H_2}^{Diff} = \frac{N_b}{2\delta^{Mem}} D_H^0 \exp\left(-\frac{E_{Diff}}{RT}\right)a(T) \quad (37)$$

In this equation, two different mechanisms arise to control the diffusion-limited flux; the first is characterized by the Sieverts driving force, and the second one depends on the simple pressure difference due to the nonideality of the system Pd−H. Splitting these two contributions into this "dual-mode" behavior, the corresponding permeances can be clearly recognized (eqs 38 and 39).

$$J_{H_2,Lim}^{Diff} = J_{H_2,Lim}^{Diff}(1) + J_{H_2,Lim}^{Diff}(2)$$
$$J_{H_2,Lim}^{Diff}(1) \equiv \pi_{H_2}^{(1)}(T, \delta^{Mem})(P_F^{0.5} - P_P^{0.5})$$
$$J_{H_2,Lim}^{Diff}(2) \equiv \pi_{H_2}^{(2)}(T, \delta^{Mem})(P_F - P_P) \quad (38)$$

$$\pi_{H_2}^{(1)}(T, \delta^{Mem}) = \frac{N_b D_H^0}{2\delta^{Mem}} \exp\left(-\frac{E_{Diff}}{RT}\right)a(T)$$
$$\pi_{H_2}^{(2)}(T, \delta^{Mem}) = \pi_{H_2}^{(1)}(T, \delta^{Mem})a(T)\left(\frac{1}{2} + \frac{b}{T}\right) \quad (39)$$

The so-obtained expression for the diffusion flux provides a possible theoretical reason why sometimes a driving force exponent n higher than 0.5 is found even for thick membranes, for which there is no doubt that the diffusion controls the process.

A3.5. Desorption-Limited Permeation. In the desorption-limited permeation, the surface coverage θ_P has to be expressed as a function of the hydrogen pressure on the feed side. If the same procedure as the one considered for the adsorption-limited

permeation is applied to the equation of the desorption flux (eq 17), eq 40 is obtained.

$$J^{\mathrm{Des}}_{\mathrm{H_2,Lim}} = \pi^{\mathrm{Des}}_{\mathrm{H_2}}(T)\left(\frac{P_\mathrm{F} - P_\mathrm{P}}{P_\mathrm{F}}\right) = \pi^{\mathrm{Des}}_{\mathrm{H_2}}(T)\frac{(\phi - 1)}{\phi}$$
$$\pi^{\mathrm{Des}}_{\mathrm{H_2}}(T) = \pi^{\mathrm{Ads}}_{\mathrm{H_2}}(T) \tag{40}$$

According to this equation, the permeance of desorption is the same as the one of the adsorption, both steps presenting, however, different characteristic driving forces.

A3.6. Adsorption−Desorption-Limited Permeation. The last case considered regards a situation in which both surface phenomena are the limiting steps at the same time (eqs 41, 42).

$$J^{\mathrm{AdsDes}}_{\mathrm{H_2,Lim}} \cong \frac{S_0}{K\sqrt{2\pi M_{\mathrm{H_2}} RT}}(1 - \theta_\mathrm{F})^2 P_\mathrm{F} - N_\mathrm{s}^2 k^0_{\mathrm{Des}} \exp\left(-\frac{2E_{\mathrm{Des}}}{RT}\right)\theta_\mathrm{F}^2 \tag{41}$$

$$J^{\mathrm{AdsDes}}_{\mathrm{H_2,Lim}} \cong N_\mathrm{s}^2 k^0_{\mathrm{Des}} \exp\left(-\frac{2E_{\mathrm{Des}}}{RT}\right)\theta_\mathrm{P}^2 - \frac{S_0}{K\sqrt{2\pi M_{\mathrm{H_2}} RT}}(1 - \theta_\mathrm{P})^2 P_\mathrm{P} \tag{42}$$

Under these conditions, where the flux of adsorption and desorption must be evidently the same (steady-state condition), θ_F and θ_P have to be expressed in terms of the hydrogen pressure on the permeate and feed, respectively. From the equilibrium relation, it can be demonstrated that θ_F and θ_P are equal, as shown in eq 43.

$$\theta_\mathrm{F} \leftrightarrow \xi_\mathrm{F} = \xi_\mathrm{P} \leftrightarrow \theta_\mathrm{P} \Rightarrow \theta_\mathrm{F} = \theta_\mathrm{P} \equiv \theta \tag{43}$$

The other relation that allows the problem to be solved is the equality of the two fluxes (eq 44), which permits expression of the surface coverage θ as a function of the hydrogen pressures (eq 45).

$$\frac{S_0(1 - \theta)^2}{K\sqrt{2\pi M_{\mathrm{H_2}} RT}}P_\mathrm{F} - N_\mathrm{s}^2 k^0_{\mathrm{Des}} \exp\left(-\frac{2E_{\mathrm{Des}}}{RT}\right)\theta^2 = N_\mathrm{s}^2 k^0_{\mathrm{Des}} \exp\left(-\frac{2E_{\mathrm{Des}}}{RT}\right)\theta^2 - \frac{S_0(1 - \theta)^2}{K\sqrt{2\pi M_{\mathrm{H_2}} RT}}P_\mathrm{P} \tag{44}$$

$$(1 - \theta)^2 \cong \frac{2N_\mathrm{s}^2 k^0_{\mathrm{Des}} \exp\left(-\frac{2E_{\mathrm{Des}}}{RT}\right) K\sqrt{2\pi M_{\mathrm{H_2}} RT}}{S_0(P_\mathrm{F} + P_\mathrm{P})} \tag{45}$$

Substituting the previous expressions into one of eqs 41 or 42, eq 46 is obtained.

$$J^{\mathrm{AdsDes}}_{\mathrm{H_2,Lim}} = \pi^{\mathrm{AdsDes}}_{\mathrm{H_2}}(T)\left(\frac{P_\mathrm{F} - P_\mathrm{P}}{P_\mathrm{F} + P_\mathrm{P}}\right) = \pi^{\mathrm{AdsDes}}_{\mathrm{H_2}}(T)\frac{\phi - 1}{\phi + 1}$$
$$\pi^{\mathrm{AdsDes}}_{\mathrm{H_2}}(T) = \pi^{\mathrm{Ads}}_{\mathrm{H_2}}(T) = \pi^{\mathrm{Des}}_{\mathrm{H_2}}(T) \tag{46}$$

This equation shows that the permeance of this case is identical to the one achieved for the adsorption and desorption steps separately considered, whereas the driving force has the same numerator but different denominator, which, therefore, characterizes each surface phenomena-limited permeation. Moreover, the form of eqs 30, 40, and 46 allows a relation between the three limiting fluxes achieved for the surface phenomena to be made explicit (eq 47).

$$\frac{1}{J^{\mathrm{AdsDes}}_{\mathrm{H_2,Lim}}} = \frac{1}{J^{\mathrm{Ads}}_{\mathrm{H_2,Lim}}} + \frac{1}{J^{\mathrm{Des}}_{\mathrm{H_2,Lim}}} \tag{47}$$

According to this equation, it is possible to evaluate directly the contributions of the adsorption- and desorption-limited fluxes to the overall adsorption−desorption-limited one. In fact, if eq 47 is written in terms of the variable ϕ, the relative weights (represented by the Greek letter α) become immediately recognizable (eq 48). The most important aspect in this relation is that the desorption step presents a contribution always higher than the one of the adsorption, this gap being progressively higher as the variable ϕ increases, that is, as the feed pressure increases with respect to the permeate one.

$$1 = \left(\frac{1}{\phi + 1}\right) + \left(\frac{\phi}{\phi + 1}\right) \Rightarrow \begin{cases} \alpha_{\mathrm{Ads}} = \dfrac{1}{\phi + 1} \\ \alpha_{\mathrm{Des}} = \dfrac{\phi}{\phi + 1} \end{cases} \tag{48}$$

Appendix B: Evaluation of the Influence of the Single Permeation Step

In this section, the way to evaluate in this paper the influence of each permeation step is described. In this frame, it must be emphasized that it is not possible to recognize an analytical overall permeation driving force because each step is characterized by its own driving force that is different, in general, from each other. Therefore, the contributions can and have to be expressed in terms of fluxes. A way to do that is suggested by the form of eq 47. In fact, in a virtual case in which the surface phenomena control the permeation, the inverse of the overall flux is expressed as the sum of the inverse limiting fluxes.

$$\frac{1}{J^{\mathrm{Overall}}_{\mathrm{H_2}}} = \frac{1}{J^{\mathrm{Ads}}_{\mathrm{H_2,Lim}}} + \frac{1}{J^{\mathrm{Des}}_{\mathrm{H_2,Lim}}} \Rightarrow 1 = \alpha_{\mathrm{Ads}} + \alpha_{\mathrm{Des}}$$
$$\alpha_{\mathrm{Ads}} \equiv \frac{\dfrac{1}{J^{\mathrm{Ads}}_{\mathrm{H_2,Lim}}}}{\dfrac{1}{J^{\mathrm{Overall}}_{\mathrm{H_2}}}} = \frac{\dfrac{1}{J^{\mathrm{Ads}}_{\mathrm{H_2,Lim}}}}{\dfrac{1}{J^{\mathrm{Ads}}_{\mathrm{H_2,Lim}}} + \dfrac{1}{J^{\mathrm{Des}}_{\mathrm{H_2,Lim}}}}$$
$$\alpha_{\mathrm{Des}} \equiv \frac{\dfrac{1}{J^{\mathrm{Des}}_{\mathrm{H_2,Lim}}}}{\dfrac{1}{J^{\mathrm{Overall}}_{\mathrm{H_2}}}} = \frac{\dfrac{1}{J^{\mathrm{Des}}_{\mathrm{H_2,Lim}}}}{\dfrac{1}{J^{\mathrm{Ads}}_{\mathrm{H_2,Lim}}} + \dfrac{1}{J^{\mathrm{Des}}_{\mathrm{H_2,Lim}}}} \tag{49}$$

Generalizing eq 49 for all of the steps considered in this paper, the following relations can be written for the *i*th step, where α indicates the level of influence of the steps (eq 50)

$$\alpha_i \equiv \frac{\dfrac{1}{J^i_{H_2,Lim}}}{\displaystyle\sum_{j=1}^{m} \frac{1}{J^i_{H_2,Lim}}} \qquad \sum_{i=1}^{m} \alpha_i = 1 \tag{50}$$

According to this expression, the higher the limiting step, the lower the influence of that step on the permeation process. This result is confirmed by the calculation plotted in Figure 9, where the steps presenting lower limiting fluxes provide most of the influence.

List of Symbols

$a(T)$	functionality with temperature in eq 36 [−]
a_0	parameter in eq 36 [−]
b	parameter in eq 23 [K^{-1}]
c_1	parameter in eqs 20 and 21 [$m^{0.5}$ $K^{0.5}$ s $kg^{-0.5}$]
D^0_H	pre-exponential factor of the atomic hydrogen diffusion coefficient [m^2 s^{-1}]
D_H	atomic hydrogen diffusion coefficient [m^2 s^{-1}]
E	activation energy [J mol^{-1}]
$F(\theta)$, $G(\theta)$, $H(\theta)$, Den(θ)	functionalities with surface coverage (eqs 12−15) [−]
J	flux [mol m^{-2} s^{-1}]
K	constant in eq 12 [−]
k^0_{Des}	pre-exponential factor of the desorption kinetic constant [m^2 s^{-1} mol^{-1}]
k_{Des}	desorption kinetic constant [m^2 s^{-1} mol^{-1}]
m	number of permeation steps
M_{H_2}	hydrogen molar mass [kg mol^{-1}]
n	driving force exponent [−]
N_s	total superficial concentration of free sites [mol_{Pd} m^{-2}]
N_b	total bulk concentration of free sites [mol_{Pd} m^{-3}]
P	pressure [Pa]
R	ideal gas constant [J mol^{-1} K^{-1}]
S_0	sticking coefficient for a Pd-based clean surface [−]
T	temperature [K]
$\bar{V}_H$	hydrogen molar fraction in the Pd-based lattice [m^3 mol_H^{-1}]
w_{HH}	hydrogen−hydrogen interaction energy [J mol^{-1}]
Y_S	Young modulus [Pa]

Greek Symbols

α	influence degree of each step [−]
δ	(membrane) thickness [m]
ΔE_{SB}	$E_{SB} - E_{BS}$ [J mol^{-1}]
ΔE_{Abs}	heat of absorption in the Pd bulk [J mol^{-1}]
ΔE_{Ads}	heat of adsorption on the Pd surface [J mol^{-1}]
ϕ	pressure ratio (eq 31) [−]
λ_{j0}	jump frequency (eqs 18, 19) [s^{-1}]
θ	surface coverage due to atomic hydrogen [mol_H mol_{Pd}^{-1}]
ξ	atomic hydrogen concentration in Pd bulk, [mol_H mol_{Pd}^{-1}]
π_{H_2}	hydrogen permeance [mol s^{-1} m^{-2} Pa^{-n} or −]
ω	parameter in eq 15 [J mol^{-1}]

Subscripts/Superscripts

F	feed side referred to
Ads	adsorption
AdsDes	adsorption−desorption
BS	bulk-to-surface
Des	desorption
Diff	diffusion
SB	surface-to-bulk
Lim	limiting (step)
Mem	membrane
P	permeate side referred to

References and Notes

(1) Dittmeyer, R.; Hollein, V.; Daud, K. Membrane reactors for hydrogenation and dehydrogenation processes based on supported palladium. *J. Mol. Catal. A: Chem.* **2001**, *173*, 135–184.

(2) Ward, T.; Dao, T. Model of hydrogen permeation behaviour in palladium membranes. *J. Membr. Sci.* **1999**, *153*, 211–231.

(3) Caravella, A.; Barbieri, G.; Drioli, E. Modelling and Simulation of Hydrogen Permeation through Supported Pd-based Membranes with a Multicomponent Approach. *Chem. Eng. Sci.* **2008**, *63*, 2149–2160.

(4) Caravella, A.; Barbieri, G.; Drioli, E. Concentration polarization analysis in self-supported Pd-based membranes. *Sep. Purif. Technol.* **2009**, *66*, 613–624.

(5) Hara, S.; Ishitsuka, M.; Suda, H.; Mukaida, M.; Haraya, K. Pressure-dependent hydrogen permeability extended for metal membranes not obeying the square-root law. *J. Phys. Chem. B* **2009**, *117*, 9795.

(6) Hu, X.; Huang, Y.; Shu, S.; Fan, Y.; Xu, N. Toward effective membranes for hydrogen separation: Multichannel composite palladium membranes. *J. Power Sources* **2008**, *181*, 135–139.

(7) Guazzone, F.; Engwall, E. E.; Ma, Y. H. Effects of surface activity, defects and mass transfer on hydrogen permeance. *Catal. Today* **2006**, *118*, 24–31.

(8) Gielens, F. C.; Tong, H. D.; Vorstman, M. A. G.; Keurentjes, J. T. F. Measurement and modeling of hydrogen transport through high-flux Pd membranes. *J. Membr. Sci.* **2007**, *289*, 15–25.

(9) Morreale, B. D.; Ciocco, M. V.; Enick, R. M.; Morsi, B. I.; Howard, B. H.; Cugini, A. V.; Rothenberger, K. S. The permeability of hydrogen in bulk palladium at elevated temperatures and pressures. *J. Membr. Sci.* **2003**, *212*, 87–97.

(10) Peters, T. A.; Stange, M.; Klette, H.; Bredesen, R. High pressure performance of thin Pd-23% Ag/stainless steel composite membranes in water gas shift gas mixtures; influence of dilution, mass transfer and surface effects on the hydrogen flux. *J. Membr. Sci.* **2008**, *316*, 119–127.

(11) Tong, J.; Matsumura, Y.; Suda, H.; Haraya, K. Experimental study of steam reforming of methane in a thin (6 μm) Pd-based membrane reactor. *Ind. Eng. Chem. Res.* **2005**, *44*, 1454–1465.

(12) Tong, J.; Su, L.; Haraya, K.; Suda, H. Thin and defect-free Pd-based composite membrane without any interlayer and substrate penetration by a combined organic and inorganic process. *Chem. Commun.* **2006**, 142–1144.

(13) Oriani, R. A. The Physical and Metallurgical Aspects of Hydrogen in Metals. In *ICCF4, Fourth International Conference on Cold Fusion*; Electric Power Research Institute: Lahaina, Maui, 1993.

(14) Zhang, Y.; Maeda, R.; Komaki, M.; Nishimura, C. Hydrogen permeation and diffusion of metallic composite membranes. *J. Membr. Sci.* **2006**, *269*, 60–65.

(15) Mejdell, A. L.; Klette, H.; Ramachandran, A.; Borg, A.; Bredesen, R. Hydrogen permeation of thin, free-standing Pd/Ag 23% membranes before and after heat treatment in air. *J. Membr. Sci.* **2008**, *307*, 96–104.

(16) Barbieri, G.; Scura, F.; Lentini, F.; De Luca, G.; Drioli, E. A novel model equation for the permeation of hydrogen in mixture with carbon monoxide through Pd−Ag membranes. *Sep. Purif. Technol.* **2008**, *61*, 217–224.

(17) Holleck, G. L. Diffusion and solubility of hydrogen in palladium and palladium−silver alloys. *J. Phys. Chem.* **1970**, *74*, 503–511.

(18) King, D. A.; Wells, M. G. Reaction mechanism in chemisorption kinetics: nitrogen on the {100} plane of tungsten. *Proc. R. Soc. London, Ser. A* **1974**, *339*, 245.

(19) Behm, R. J.; Christmann, K.; Ertl, G. Adsorption of hydrogen on Pd(100). *Surf. Sci.* **1980**, *99*, 320.

JP1006582